Vertical Wind Shear Effects on Kelvin Wave-CISK Modes: Possible Relevance to 30 ~ 60 Day Oscillations

HOCK LIM[1] C.-P. CHANG[1] AND TIAN-KUAY LIM[2]

(Received 28 January 1991; Revised 27 March 1991)

ABSTRACT

Several numerical model simulations (Hayashi and Sumi, 1986; Lau and Peng, 1987) reported generation of eastward propagating equatorial disturbances which appear to be model analogs of the observed 30~60 day oscillations. Kelvin wave-CISK has been proposed as a possible mechanism for driving these simulated disturbances (Lau and Peng, 1987; Chang and Lim, 1988). However, model and theoretical wave-CISK disturbances all propagate faster than the observed oscillations. In this paper, we investigate whether the "Doppler shifting" effect by a mean wind may adequately slow down the wave-CISK modes. In addition, the effect of vertical mean wind shear on their stability is also studied. The model and solution methods of this paper is adopted from Lim *et al.* (1990). Mean winds with a linear shear in the pressure coordinate are considered. It is found that a westerly shear tends to stabilize the Kelvin wave-CISK modes while an easterly shear tends to enhance their instability. The wave-CISK modes are "Doppler shifted" by the mean winds, but to only about 60 ~ 70% of the vertical-averaged mean wind speed. Based on the climatological equatorial mean winds, growth rate and propagation speed of the Kelvin wave-CISK modes are estimated for various longitudes. With the mean wind effect, the Kelvin wave-CISK modes take about 35~40 days to travel around the equatorial belt. Their growth rate is largest over the Indian Ocean and western Pacific Ocean where increased activity of convective clouds associated with the oscillations are often reported.

1. INTRODUCTION

Many theories have been proposed for the 30 ~ 60 day oscillations first observed by Madden and Julian (1972). Chang (1977) interpreted the phenomena as a slow mode of forced Kelvin waves in which heating is balanced by dissipation. This mode of Kelvin waves, in contrast to the usual gravity-type of Kelvin wave, have a deep circulation trapped in the troposphere, and propagates with a phase speed of about 10 m/s. Later theories tended to explore

[1] *Department of Meteorology, Naval Postgraduate School, Monterey, U. S. A.*

[2] *Meteorological Service Singapore, Republic of Singapore*

alternative mechanisms, such as periodic equatorial forcing, hydrological cycle, air-sea thermal exchange, etc. However, none of such mechanisms provides for a natural explanation of the eastward propagation of the observed oscillations.

Interests in the Kelvin wave interpretation were revived by numerical simulation studies by Hayashi and Sumi (1986) and Lau and Peng (1987). In the former study with a general circulation model, eastward propagating disturbances were obtained which could be regarded as model analogs of the observed oscillations, except that the propagation speed is slightly too fast. Lau and Peng (1987) used a 5-level global model with wave-CISK parameterization and obtained similar disturbances, but of a more well defined structure. Again the propagation speed is faster than observed. The disturbances has a "wavenumber one" structure with a narrow axis of ascending motion which tilts backward with height. The circulation ahead of the axis is deeper and stronger than the circulation behind the axis. They interpreted the disturbances as "mobile" wave-CISK modes.

Chang and Lim (1988) presented a linear theory of Kelvin wave-CISK. Depending on the vertical heating profile, they obtained solutions representing propagating Kelvin wave-CISK modes and stationary wave-CISK modes. Their linear Kelvin wave-CISK modes give a satisfactory explanation of the general characteristics of Lau and Peng's (1987) disturbances. In particular, Gaussian wave packages constructed by super-positioning the linear Kelvin wave-CISK modes reproduce very well the characteristics of the disturbances, including the east-west asymmetric structure. These Kelvin wave-CISK modes can be considered, in the context of the five-level model, to be generated through the interactions of a faster and a slower vertical normal modes in the following manner. The heating associated with concentrated ascending motion excites both of the modes. The faster mode which has a deeper circulation propagates ahead of the source while the slower mode which has a shallower circulation trails behind the source. The shallower mode has more influence on the lower-level flow and so it controls the CISK heating. The deeper mode, when leading the slower mode by an appropriate distance (or phase), will have the CISK heating acting in its warm region, and hence gains energy for growth. The fact that the Kelvin wave-CISK mode grows via the faster mode also explains why the circulation ahead of the rising motion tends to be the stronger.

There are two difficulties in the linear wave-CISK theory. The first is the usual "short wave explosion" problem of gravity wave-CISK. According to the theory, the most unstable mode should be in the cumulus scale rather than in the "wavenumber-one" scale of the simulated disturbances. Wang and Rui (1989) considered the coupling of the Kelvin wave-CISK modes with Rossby waves through Ekman-type boundary layer effects and obtained linear coupled wave-CISK modes which are most unstable at wavenumber one or two. This additional mechanism is worthy of further study, but it does not really address

the issue at hand. There was no Ekman-type forcing in Lau and Peng's (1987) model, so the new mechanism cannot be the reason of the wavenumber-one structure of their disturbances. Two recent works have examined the nonlinear dynamics for an explanation of the organisation. Itoh (1989) studied several external nonlinear constraints (including "positive-only" heating) which might limit culmulus scale development in numerical models. He concluded that a dry region over wide areas in the tropics is required to suppress cumulus-scale development due to CISK. In a re-examination of the wave-CISK mechanism, Lim, Lim and Chang (1990, hereinafter referred to as LLC) demonstrated the existence of nonlinear unstable modes. In such a wave-CISK mode, all wavenumber components lock in phase with each other, resulting in a wavenumber-one structure which grows exponentially and propagates steadily without change of shape. Their study suggests that the low frequency eastward propagating disturbances simulated in the numerical models are probably a consequence of the nonlinear wave-CISK dynamics.

Another difficulty of the wave-CISK theory concerns the propagation speed of Kelvin wave-CISK disturbances. So far, model and theoretical studies have obtained propagation speed of $15 \sim 20\ m/s$, which implies a period of $20 \sim 30$ days. It is possible to bring in other mechanisms to slow down the Kelvin wave-CISK modes. For instance, some of Wang and Rui's (1989) coupled Kelvin-Rossby modes propagate as slow as $5\ m/s$. In this paper, we shall examine a simple effect for slowing down the Kelvin wave-CISK modes: advection by a mean wind. This "Doppler shifting" was in fact invoked by Chang (1977) when interpreting the observed oscillations in terms of his viscous Kelvin waves. In most models, such as the one we shall adopt for this study, the case of a uniform mean wind is trivial, as the propagation speed of the modes will be simply "shifted" by the mean wind speed. We shall therefore consider the simplest nontrivial case of a mean wind with a linear vertical shear (in p-coordinate). The vertical wind shear may also be expected to affect the stability of the modes besides Doppler shifting their propagation speed.

2. THE MODEL

We adopt the following two-dimensional p-coordinate model for this study:

$$\begin{aligned} &\frac{\partial u}{\partial t} + U(p)\frac{\partial u}{\partial x} + \omega\frac{dU}{dp} + \frac{\partial \phi}{\partial x} = D_u \frac{\partial^2 u}{\partial x^2} \\ &\frac{\partial}{\partial t}\frac{\partial \phi}{\partial p} + U(p)\frac{\partial}{\partial x}\frac{\partial \phi}{\partial p} + \sigma\omega = -\frac{RQ}{c_p p} + D_\phi \frac{\partial^2}{\partial x^2}\frac{\partial \phi}{\partial p} \\ &\frac{\partial u}{\partial x} + \frac{\partial \omega}{\partial p} = 0 \end{aligned} \tag{1}$$

where $U(p)$ is the mean wind, u the wind perturbation, ϕ the geopotential perturbation, ω the p-velocity, σ the static stability parameter, R the gas constant,

c_p the specific heat of air at constant pressure, and D_u and D_ϕ are constant diffusion coefficients. The term Q represents CISK heating parameterized in the standard way:

$$Q(x,p,t) = mLq_c^*\,\eta(p)[-\omega_c(x,t)] \tag{2}$$

where m is the moisture availability factor, L the latent heat, q_c^* the specific humidity at the condensation level, $\eta(p)$ the normalised vertical heating profile (i.e., $\int_0^{p_s}\eta(p)\,dp = 1$, where p_s denotes the surface pressure level), ω_c the p-velocity at the condensation level, and $[\varphi]$ a function of φ which is equal to φ when $\varphi > 0$ and vanishes otherwise.

The boundary conditions for (1) are

$$\omega = 0 \qquad \text{at} \qquad p = 0 \tag{3a}$$

and

$$\frac{\partial\phi}{\partial t} + U(p)\frac{\partial\phi}{\partial x} = \frac{1}{\rho_s}\omega \qquad \text{at} \qquad p = p_s \tag{3b}$$

where ρ_s is the density of air at the lowest pressure level.

We shall specify the mean wind to be $U(p) = U_t(1 - p/p_s)$ where U_t is a constant representing the wind at the top of the atmosphere. The results of integration can be easily applied to situation where the surface wind $U(p_s) = U_s \neq 0$. Eqs. (1)~(3) do not change their form when subjected to the transformation $(x,t) \to (x - U_s t, t)$. This means that solutions for $U_s \neq 0$ may be obtained by simply moving the corresponding solution with $U_s = 0$ with the constant speed U_s.

As explained in LLC, the numerical scheme used for solving Eqs. (1)~(3) should minimize numerical dispersion of the Kelvin waves, and conserve energy for each individual wavenumber components when the CISK heating, vertical wind shear, and damping effects are turned off. The above requirements are met by the following J-level, M-wave energy-conserving spectral model:

$$\begin{aligned}
\frac{d}{dt}u_{m,j-} &= -iU\,k_m\,u_{m,j-} - ik_m\,\phi_{m,j-} \\
&\quad - \frac{1}{2}\left(\frac{dU}{dp}\right)_{j-}(\omega_{m,j-1} + \omega_{m,j}) - D_u\,k_m^2\,u_{m,j-} \\
\frac{d}{dt}\delta\phi_{m,j} &= -iU\,k_m\,\delta\phi_{m,j} - \sigma_j\,\omega_{m,j} - \frac{RQ_{m,j}}{c_p\,p_j} - D_\phi\,k_m^2\,\delta\phi_{m,j} \\
\frac{d}{dt}\phi_{m,J-} &= -iU\,k_m\,\phi_{m,J-} + \frac{1}{\rho_s}\omega_{m,J} \\
\delta\omega_{m,j-} &= -ik_m\,u_{m,j-}
\end{aligned} \tag{4}$$

where $\varphi_{m,j}$ denotes the amplitude of the mth wave component of the variable φ at the jth level, $j-$ denotes $j-/2$, and $\delta\varphi_{m,j}$ denotes $(\varphi_{m,j+1/2} - \varphi_{m,j-1/2})/\Delta p$.

Note that the prognostic equation for $\phi_{m,J-}$ (lower boundary condition equation) includes the term $\omega_{m,J}$ rather than $\omega_{m,J-}$ in order to conserve energy. During integration, it is necessary to compute $[\omega_c]$ in the spatial domain and then transform it to obtain $Q_{m,j}$.

From (4), we may derive the following equation for the variation of the total energy of the system:

$$\begin{aligned}
&\frac{d}{dt}\sum_m \left\{ \sum_{j=1}^{J} \frac{\Delta p}{2} u^*_{m,j-} u_{m,j-} + \sum_{j=1}^{J-1} \frac{\Delta p}{2\sigma_j} \delta\phi^*_{m,j} \delta\phi_{m,j} + \frac{\rho_s}{2} \phi^*_{m,J-} \phi_{m,J-} \right\} \\
&= \sum_m \sum_{j=1}^{J-1} -\frac{R\Delta p}{2c_p p_j \sigma_j} \left[\delta\phi^*_{m,j} Q_{m,j} + \delta\phi_{m,j} Q^*_{m,j} \right] \\
&\quad + \sum_m \sum_{j=1}^{J} -\frac{\Delta p}{4} \left(\frac{dU}{dp} \right)_{j-} \left[\left(\omega^*_{m,j-1} + \omega^*_{m,j} \right) u_{m,j-} + \left(\omega_{m,j-1} + \omega_{m,j} \right) u^*_{m,j-} \right] \\
&\quad - \sum_m \sum_{j=1}^{J} \Delta p D_u k_m^2 u^*_{m,j-} u_{m,j-} \\
&\quad - \sum_m \sum_{j=1}^{J-1} \Delta p D_\phi k_m^2 \delta\phi^*_{m,j} \delta\phi_{m,j}
\end{aligned} \tag{5}$$

where φ^* denotes the complex conjugate of φ. The first term on the right hand side of (5) represents the energy generation rate due to CISK heating, the second that due to vertical advection across shear in the mean wind, the last two represent the energy dissipation rates due to damping effects. The individual terms were totalled separately during computations to provide a diagnostic of the energy exchange processes involved in the development of the wave-CISK modes.

3. EFFECTS OF VERTICAL WIND SHEAR

The solution procedure adopted in this study is exactly the same as in LLC. The model parameters are specified as follows: $J = 5$, $M = 64$, $m = 1$, and $\Delta t = 5$ *minutes*. All integrations start from an initial condition representing a Kelvin wave package which propagates steadily eastward with a speed of 36.14 m/s. The wave package is constructed so that the vertical velocity at 900 mb, ω_{900}, has a Gaussian profile with of a half width of 12° latitude. With an appropriate vertical heating profile, a Kelvin wave-CISK modes emerges after an adjustment period of a few days. The mode grows exponentially with time, and propagates steadily eastward without change of shape. The growth rate of the mode is calculated from the gradient of the plot of its total energy (in logarithmic scale) against time.

We shall denote the relative heating rate at the 1000, 800, 600, 400, and 200 mb levels by the symbols ξ_{1000}, ξ_{800}, ξ_{600}, ξ_{400}, and ξ_{200}. The vertical heating profile parameter ζ of Eq (2) is given by normalizing the parameters ξ_s. Our first set of results was obtained with the $\xi_{1000} = \xi_{200} = 0$, $\xi_{800} = 1$, $\xi_{600} = 2$, and $\xi_{400} = 0.5$. The diffusion coefficients $D_u = D_\phi = 10^5\ m^2/s$. Without a mean wind, this heating profile will produce a Kelvin wave-CISK mode with a speed of about 16 m/s. To clearly highlight the horizontal advection effect of the mean wind alone, we carried out the integrations twice, first with the $\omega\, dU/dp$ term in the first equation of (1) turned off, and then with it restored. The growth rates and propagation speeds of the modes are plotted against U_t in Figures 1a and b, respectively, where the open circles ° (solid circles •) denote the model results for cases without (with) the $\omega\, dU/dp$ term.

The open-circle curve of Figure 1a shows that the horizontal advection effect of a westerly shear is to stabilise the Kelvin wave-CISK modes while that of a easterly shear is to enhance its instability. This may be understood by the following reasoning. Kelvin wave-CISK modes have a backward tilting axis of ascending motion. This tilt enables the CISK heating to act on the warm air just ahead of the axis of ascending motion, and hence renders the modes unstable. The horizontal advection effect of a vertical wind shear is such that a westerly shear tends to reduce the backward tilt of the axis while an easterly shear tends to enhance the tilt. Thus the growth will be affected accordingly. There is a kink in the growth rate near $U_t = -25\ m/s$. The reason for this kink is not understood.

The open-circle curve of Figure 1b shows that the propagation speed of the Kelvin wave-CISK modes is affected by the mean wind. The average mean wind through the depth of the atmosphere is $U_t/2$. However, the gradient of the curve is about $1/3.5$, which indicates that the horizontal advection effect on the propagation speed is only about 60% of the average mean wind through the depth of the atmosphere. If we consider the fact that the Kelvin wave-CISK modes extend generally up to only about 200 mb, the average mean wind through the depth of the mode is then $2U_t/5$, and the effectiveness of the horizontal advection effect increases to about 70%. The 60% ~ 70% effectiveness of the "Doppler shifting" may be explained again in terms of the fast-slow vertical mode interaction mechanism revealed in the analysis of linear Kelvin wave-CISK (Chang and Lim, 1988). As the lower-level convergence field is controlled more by the slower mode which has a shallower circulation, only the lower-level mean wind may be expected to be effective in advecting the source of wave-CISK energy. From this point of view, the 60 ~ 70% effectiveness figure appears understandable.

The solid-circle curves of Figures 1a, b show the total mean wind effects, horizontal advection as well as vertical advection across vertical wind shear ($\omega\, dU/dp$). The vertical cross-shear advection effect in general acts in opposi-

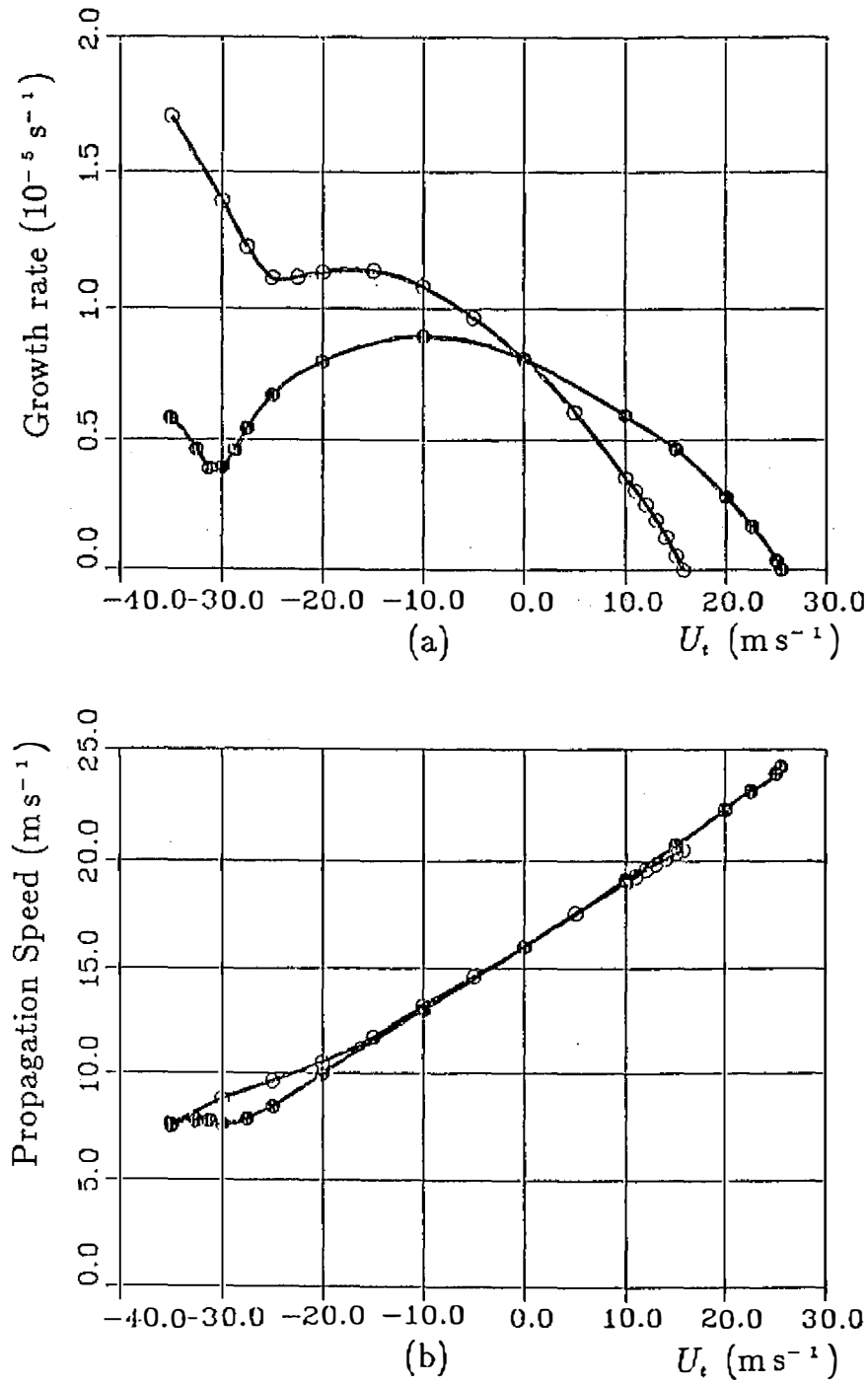

Fig. 1. (a) Growth rate and (b) propagation speed of nonlinear Kelvin wave-CISK modes in vertical mean wind shear. • indicates values obtained in computations using the complete equations and ○ indicates values obtained in computations neglecting the $\omega\, dU/dp$ term.

tion to the horizontal advection effect, i.e., it renders the modes less unstable in an easterly shear and more unstable in a westerly shear. The vertical shear term contributes a term $-u\omega\, dU/dp$ to the energy equation. We may assume that much of the contribution of this term comes from the vigorous ascending motion within the narrow axis, where $u < 0$ and $\omega < 0$. The backward tilt of the axis means that $-u\omega$ is negative. In an easterly shear, $dU/dp > 0$ and $-u\omega\, dU/dp < 0$, implying a sink on the perturbation energy of the wave-CISK mode. Vertical advection across an easterly shear therefore tends to stabilize the mode. Conversely, in a westerly shear, $dU/dp < 0$ and vertical advection across a westerly shear tends to destabilize the mode. This vertical advection effect is however weaker than the horizontal advection effect. The total influence of a vertical wind shear on the grow rate can be considered to be basically due to the horizontal advection effect, but moderated by the vertical advection effect. The solid-circle curve in Figure 1b indicates that although the vertical advection effect significantly affects the growth rate, its influence on the propagation speed is negligible.

Figures 2a, b show the growth rate and propagation speed of another Kelvin wave-CISK mode in a sheared mean wind. The heating profile for the mode is $\xi_{1000} = \xi_{200} = 0$, $\xi_{800} = 1$, $\xi_{600} = 2$, and $\xi_{400} = 1$. Without a mean wind, the speed of this mode is about 18 m/s. The total mean wind effect is included. The stabilizing effect of a westerly shear and the destabilizing effect of an easterly shear is again clearly illustrated. The kink in the growth rate occurs at $U_t = -18$ m/s. A shift in the propagation speed accompanies the kink in the growth rate. The average gradient of the propagation speed curve again implies a 60 $\sim$ 70% effectiveness of the mean wind in Doppler shifting the propagation speed of the wave-CISK mode.

The longitude-height profiles of the Kelvin wave-CISK modes in vertical shear are shown in Figures 3a$\sim$j for $U_t = -35$, -30, -25, -20, -15, -10, -5, 0, 5, and 10 m/s respectively. In agreement with LLC, the overall structure of a mode appears to be largely characterized by its growth rate. The more unstable modes have a narrower longitudinal extent and exhibit stronger east-west asymmetry. The near neutral modes (e.g., the mode for $U_t = 10$ m/s) has a nearly symmetrical structure like a free Kelvin wave package. The axis of ascending motion may be seen to broaden significantly when the growth rate becomes small.

4. POSSIBLE RELEVANCE TO 30 $\sim$ 60 DAY OSCILLATIONS

In this section, we present a preliminary estimate of the effects of the equatorial climatological mean zonal wind on the Kelvin wave-CISK modes. The basic data is obtained from Newell *et al.* (1972). The Dec–Feb and Jun–Aug mean winds at various pressure levels for 180°, 120° W, 60° W, 0°, 60° E, and 120° E, are read off their Figure 3.9 and Figure 3.10 respectively. Least

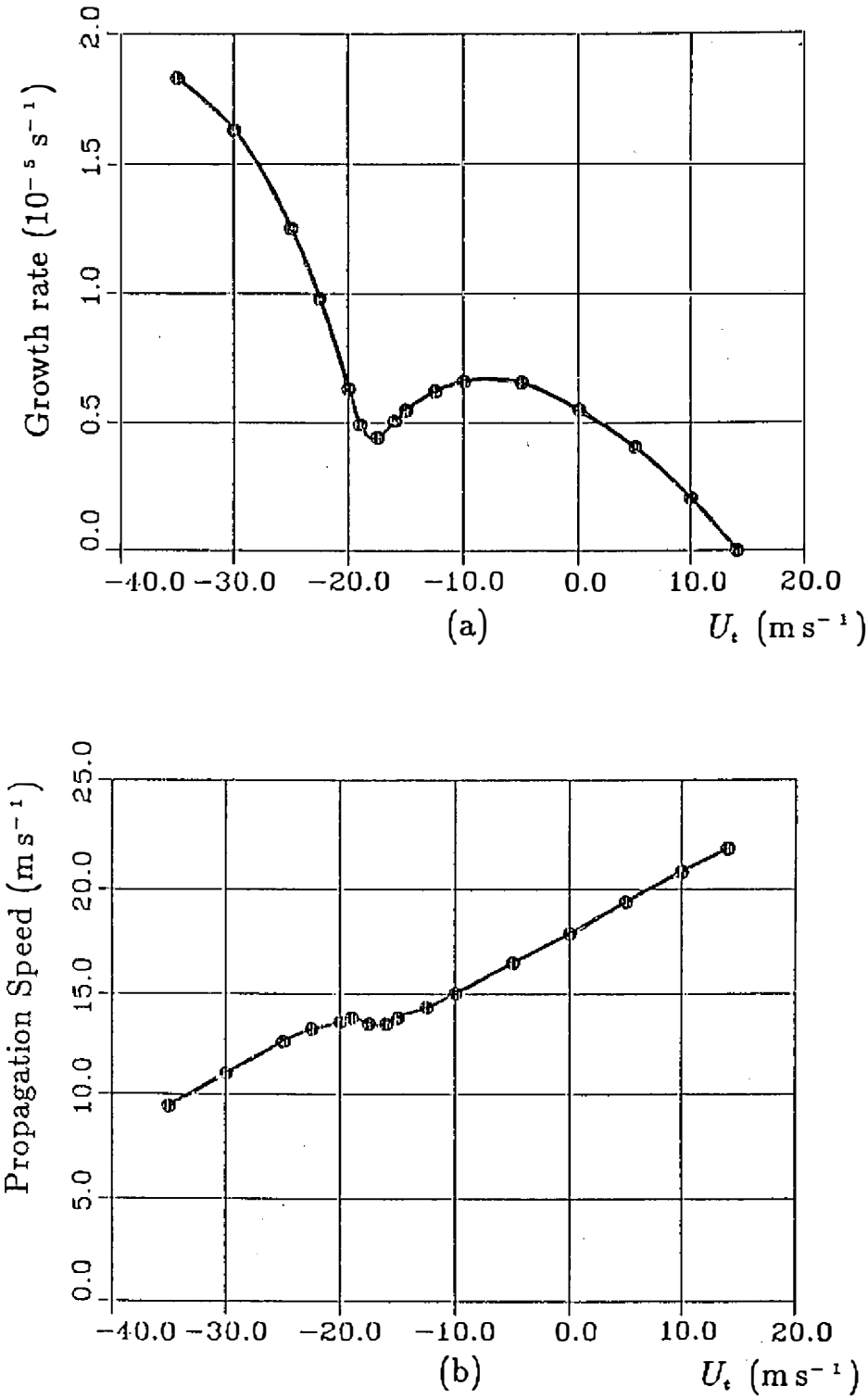

Fig. 2. Same as Figure 1 but for a different vertical heating profile.

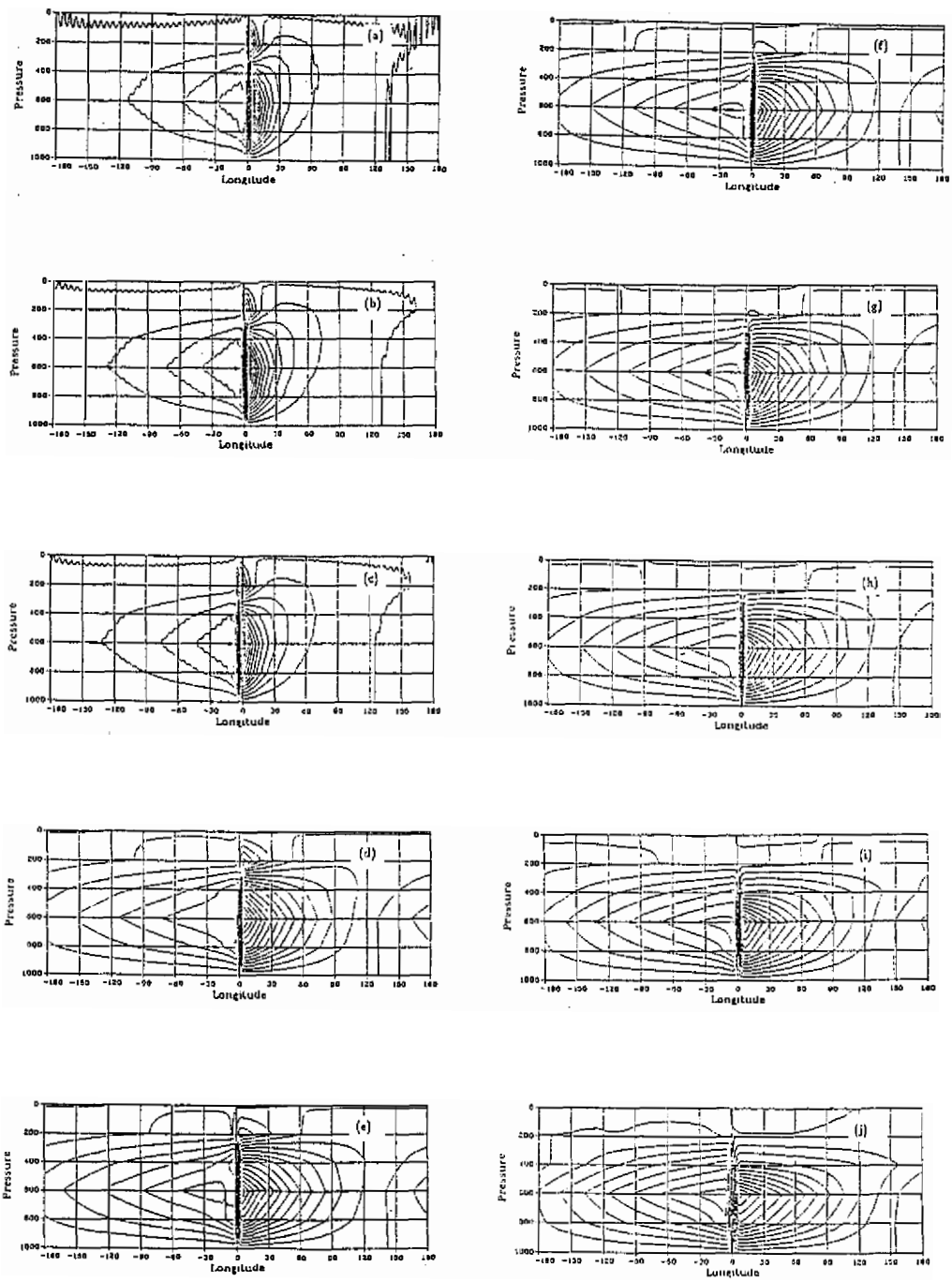

Fig. 3. The structure of the Kelvin wave-CISK modes in vertical mean wind shear: (a) $U_t = -35\,\mathrm{m\,s^{-1}}$; (b) $U_t = -30\,\mathrm{m\,s^{-1}}$; (c) $U_t = -25\,\mathrm{m\,s^{-1}}$; (d) $U_t = -20\,\mathrm{m\,s^{-1}}$; (e) $U_t = -15\,\mathrm{m\,s^{-1}}$; (f) $U_t = -10\,\mathrm{m\,s^{-1}}$; (g) $U_t = -5\,\mathrm{m\,s^{-1}}$; (h) $U_t = 0$; (i) $U_t = 5\,\mathrm{m\,s^{-1}}$; (j) $U_t = 10\,\mathrm{m\,s^{-1}}$. This modes have vertical heating profile (0, 1, 2, 1, 0) at the (1000, 800, 600, 400, 200) mb-levels.

square straight lines (in p-coordinate) are then fitted through the data for each longitude to obtain the values for U_s and U_t. The growth rate of a Kelvin wave-CISK mode for a given U_t may then be read off Figure 1a or Figure 2a, and its propagation speed obtained by reading off the appropriate value from Figure 1b or Figure 2b and then adjusting it with U_s. This is carried out for all the four possible combinations for the two seasonal periods (Dec–Feb and Jun–Aug) and the two heating profiles represented in Figures 1 and 2. The four sets of results are then averaged, giving the final estimate as shown in the following table:

Longitude	180	120W	60W	0	60E	120E
Speed($m\ s^{-1}$)	11.0	13.0	11.0	8.5	16.5	15.0
Growth Rate(day^{-1})	0.36	0.48	0.29	0.52	0.67	0.67

With the above estimated propagation speeds, a Kelvin wave-CISK mode would propagate around the equatorial belt once in every 35 $\sim$ 40 days, within the range of the observation period. However, we should note that the estimated propagation speed is highest (about 16 m/s) over the Indian Ocean and western Pacific Ocean. This is not supported by observations.

The growth rate is highest over the Indian Ocean and the western Pacific Ocean. This is mainly due to the presence of the easterly jet in this region which gives rise to a strong easterly vertical shear. This regional preference is in good agreement with observations, where increased activity of convective clouds associated with the oscillations are often reported.

5. DISCUSSIONS

From this study, we may draw the following conclusions about the effects of a mean wind with a vertical shear:

(1) A westerly shear tends to stabilize the Kelvin wave-CISK modes while an easterly shear tends to enhance its instability.

(2) The propagation speed of a Kelvin wave-CISK modes is "Doppler shifted" by the mean wind, more effectively by the lower-level mean winds than the upper-level mean winds.

(3) The Kelvin wave-CISK modes in climatological equatorial mean winds take about 35 $\sim$ 40 days to propagate round the equatorial belt. This period falls within the range of the observed cycle of the 30 $\sim$ 60 days oscillations. However, the variation of the estimated propagation speed with longitude does not agree with the observed variation.

(4) The easterly jet over the Indian and wester Pacific Ocean significantly enhances the growth rate of the Kelvin wave-CISK modes. Convective

cloud clusters associated with the oscillations are observed in this region. Longitudinal variation in the strength of the oscillations is often attributed to variations in the sea surface temperature. Our results indicate that the vertical shear of the mean wind may be a complementary factor.

To attempt an interpretation of the more detailed characteristics of the observed 30 ~ 60 day oscillations based on the Kelvin wave-CISK theory, we need to extend the theory in two directions. Firstly, the vertical heating profile has been specified in all the wave-CISK model or theoretical studies. In reality, the vertical heating profile probably varies with the development of a convective system, leading finally to a quasi-neutral mature state. This mutual adjustment process between the convective system and the environment is excluded by the basic wave-CISK formulation of our study. To extend the theory along this direction would require the replacement of the wave-CISK parameterization with some more sophisticated methods of incorporating the moist convection process. Secondly, our theory has been restricted to Kelvin waves alone. In the atmosphere, a Kelvin wave-CISK mode can be expected to excite many other wave modes in its eastward propagation just like a ship makes waves sailing through water. These excited wave motions may slightly modify the overall appearance of the Kelvin wave-CISK mode or may slow it down through wave-drag effect. Furthermore, a direct coupling between the Kelvin wave-CISK modes and Rossby waves may also be possible through other mechanisms such as an Ekman-type boundary layer effects (Wang and Rui, 1989). An extension of the Kelvin wave-CISK theory to allow for passive excitation of (or active coupling with) other wave modes will probably bring out many detailed three-dimensional features of the unstable modes for comparison with observations.

Acknowledgements. This work was supported by the National Science Foundation, Division of Atmospheric Sciences, under Grant ATM-9106495. The visit of the first author to the Naval Postgraduate School was sponsored by the G.J. Haltiner Research Chair Program.

REFERENCES

Chang, C.-P., 1977: Viscous internal gravity waves and low-frequency oscillations in the tropics. *J. Atmos. Sci.*, **34**, 901–910.

____, and H. Lim, 1988: Kelvin wave-CISK: a possible mechanism for the 30~50 day oscillations. *J. Atmos. Sci.*, **45**, 1709–1720.

Hayashi, Y.-Y., and A. Sumi, 1986: The 30~40 day oscillations simulated in an "aqua planet" model. *J. Meteor. Soc. Japan*, **64**, 451–467.

Itoh, H., 1988: The mechanism for the scale selection of tropical intraseasonal oscillations. Part I: Selection of wavenumber 1 and the three-scale structure. *J. Atmos. Sci.*, **46**, 1779–1798.

Lau, K.M., and L. Peng, 1987: Origin of low frequency (intraseasonal) oscillations in the tropical atmosphere. Part I. The basic theory. *J. Atmos. Sci.*, **44**, 950–972.

Lim, H., T.K. Lim, and C.-P. Chang, 1990: Re-examination of wave-CISK theory: existence and properties of nonlinear wave-CISK modes. *J. Atmos. Sci.*, **47**, 3078–3091.

Madden, R.A., and P.R. Julian, 1972: Description of global-scale circulation cells in the tropics with a 40~50 day period. *J. Atmos. Sci.*, **29**, 1109–1123.

Newell, R.E., J.W. Kidson, D.G. Vincent, and G.J. Boer, 1972: *The General Circulation of the Tropical Atmosphere*. The MIT Press, Cambridge, Massachusetts.

Wang, B., and H. Rui, 1989: Some dynamic aspects of the equatorial intraseasonal oscillations. Paper presented in the International Conference on East Asia and Western Pacific Meteorology and Climate, 6~8 July 1989, Hong Kong.

垂直風切對 Kelvin Wave-CISK 的影響：與 30～60 天振盪的可能關係

Hock Lim 張智北 Tian-Kuay Lim

摘要

有些數值模擬（ Hayashi and Sumi, 1986; Lau and Peng, 1987 ）的結果中發現有向東傳送的赤道擾動，其若干性質與觀測到的 30～60 天振盪相似。Lau and Peng （1987）及 Chang and Lim （1988） 曾建議 Kelvin Wave-CISK 可能是此類模擬之擾動的發展機制。但是 KWC 理論上和模式中的擾動都比觀測的擾動傳送速度爲快。本文主要目的在探討平均風場造成的都卜勒效應可否足以減慢理論上 KWC 的傳送速度，並同時研究垂直向平均風切對穩定度的影響。本文使用我們（Lim et al., 1990）的模式及求解方法，加上在氣壓坐標內的線性垂直平均風切。結果顯示西風風切會增加 KWC 波的穩定度，東風風切則減少其穩定度。波傳送的速度確會受到平均風的都卜勒效應，但影響程度約爲垂直平均的 60～70%。根據赤道地區氣候平均風資料，我們計算出在不同經度 KWC 波的傳送速度和不穩定成長率，結果顯示 KWC 波用約 35～40 天環繞赤道一週，此周期已在觀測的範圍之內。波的成長率在印度洋和西太平洋最大，這些也是觀測到的擾動對流經常增長的區域。